Iranian Journal of Fisheries Sciences
http: doi.org/ 10.22092/ijfs.2026.135478 2026, 25(3) 467-494

Research Article

Development of Zein/Fucoidan/Tio₂ nanocomposite films from *Sargassum tenerrimum* for food packaging

Chahkhoozadeh S.[1], Akhondzadeh Basti A.[2], Tala M.[3*], Anvar A.A.[4], Khanjari A.[2]

1 Department of Science and Research, Islamic Azad University, Qeshm Branch, Qeshm, Iran
2 Department of Food Hygiene and Control, Faculty of Veterinary Medicine, University of Tehran, Tehran, Iran
3 Department of Fisheries, Islamic Azad University, Qeshm Branch, Qeshm, Iran
4 Department of Food Hygiene, Faculty of Veterinary Medicine, Islamic Azad University, Science and Research Branch, Tehran, Iran
*Correspondence:Talaazad29@gmail.com

Keywords

Titanium dioxide,
Sargassum tenerrimum,
Nanocomposite,
Fucoidan

Article info

Received: January 2025
Accepted: June 2025
Published: May 2026

Abstract

This study aimed to create a novel biodegradable film by incorporating biosynthesized titanium dioxide (TiO_2) nanoparticles into a zein/fucoidan matrix for food packaging applications. TiO_2 nanoparticles were synthesized using *Sargassum tenerrimum* extract and confirmed using UV-Vis spectroscopy and dynamic light scattering (DLS). The antioxidant activity was assessed by DPPH assay, showing an IC_{50} value of 0.347 mg/mL. The prepared films were evaluated for thickness, solubility, oxygen permeability, water vapor permeability, and mechanical properties. Zein films exhibited the highest values for solubility, elongation at break, oxygen permeability, and tensile strength, whereas the lowest values were recorded for the Zein + 5% Fucoidan + 2.5% TiO_2 nanocomposite ($p \leq 0.05$). FTIR, DSC, and XRD results confirmed interplays between TiO_2 nanoparticles and the carbonyl and carboxyl functional groups within the nanocomposite matrix. The study acknowledges that further investigations are needed to assess long-term storage stability and performance in real food systems. This study introduces a novel bioactive nanocomposite film with enhanced barrier and mechanical properties, distinguishing it from conventional biodegradable films. The Zein + 5% Fucoidan + 2.5% TiO_2 nanocomposite was identified to have the optimal formulation, demonstrating superior performance and having potential for application in food preservation.

Introduction

The expanding concerns about the environment are due to plastic damage and the growing demand for safe, sustainable food packaging, and have driven extensive research into biodegradable and bioactive films. Among various biopolymers, zein—a hydrophobic protein derived from corn—has attracted attention because of its great ability in forming films, water vapor barrier features, and UV resistance, making it suitable for packaging moisture-sensitive foods (Dukuzeyesu *et al*., 2020). However, pure zein films are often brittle and lack sufficient antimicrobial activity, which limits their real usages within the food industry (Qu *et al*., 2019). To manage these impediments, analysts have investigated the incorporation of bioactive polysaccharides like fucoidan, a sulfated polysaccharide extracted from brown algae, into protein-based matrices. Fucoidan is recognized for its potent antioxidant and antimicrobial features, attributed to its high sulfate quantity and radical scavenging capacity. Incorporating fucoidan into edible films not only enhances their flexibility and mechanical strength but also imparts bioactive functionalities that can inhibit microbial growth and oxidative degradation on food surfaces. For instance, gelatin/fucoidan films have demonstrated improved thermal stability, antioxidant activity, and antibacterial properties, supporting their application as bioactive edible films in food packaging (Pouralkhas *et al*., 2023). Similarly, zein/fucoidan nanoliposome systems have shown superior encapsulation efficiency, physicochemical stability, and enhanced antioxidant activity, further validating the potential of fucoidan in functional packaging frameworks (Chen *et al*., 2024). Thus, the present paper aims to fabricate and characterize a novel zein/fucoidan nanocomposite film incorporated with green-synthesized TiO_2 nanoparticles.

In addition to biopolymer blending, the integration of inorganic nanoparticles such as titanium dioxide (TiO_2) has emerged as a promising approach to further enhance the physicochemical and antimicrobial properties of edible films. TiO_2 is well-known for its photocatalytic properties. Under UV irradiation, they generate reactive oxygen species (ROS), which are highly effective in inactivating a wide range of bacteria (Li *et al*., 2025). Adding nano-TiO_2 to biopolymer films such as zein/chitosan or PVA/cellulose nanocrystals significantly improves mechanical potency, water vapor and UV barrier properties, and antibacterial activity, confirming its value in active packaging (Qu *et al*., 2019; Nguyen and Lee, 2022). Notably, highly dispersible TiO_2 nanoparticles have been shown to increase the tensile strength and thermal stability of zein-based films, while providing important antibacterial impacts against both Gram-negative and Gram-positive bacteria—especially under UV light (Qu *et al*., 2019). Despite these advances, the specific combination of zein and fucoidan with TiO_2 nanoparticles remains largely unexplored. While several investigations have studied the impacts of TiO_2 on the properties of protein- or polysaccharide-based films, and others have examined the bioactivity of fucoidan-containing films, there is a clear research gap regarding the synergistic effects of all three components

in a single nanocomposite system (Chen *et al*., 2024). No reports have systematically evaluated zein/fucoidan/TiO_2 nanocomposite films for their structural, antioxidant, and antimicrobial performance in food packaging applications. We hypothesize that the synergistic combination of hydrophobic zein, bioactive fucoidan, and photocatalytic TiO_2 will enhance the film's UV-blocking, antimicrobial, and mechanical properties, offering a sustainable and multifunctional solution for dynamic food packaging.

Materials and methods

Materials

Sargassum tenerrimum (brown algae) was collected from the shores of the Persian Gulf and authenticated by a marine botanist at the Herbarium of the Faculty of Science, University of Tehran, Iran. Corn flour was sourced from Gulha Food Industry, Iran. All laboratory chemicals, including analytical-grade ethanol, acetone, calcium chloride, and other reagents, were bought from Merck, Germany, and there was no further purification of the chemicals when used.

Preparation of fucoidan from Sargassum tenerrimum algae

To extract fucoidan, the collected algae were thoroughly washed using distilled water in order to clear sediments and foreign materials. The cleaned algae were shade-dried at ambient temperature (25±2°C) for 48 h and subsequently powdered using an electric mill. A total of 20 g of dry algal powder was suspended in 200 mL of 80% (v/v) ethanol and stirred for 2 h magnetically at 300 ×g at room temperature (25±2°C) to clear pigments and proteins. The suspension was then filtered, and the residue was washed with acetone and centrifuged at 5000 ×g at 4°C for 10 min. The dried algae were extracted with distilled water at a ratio of 1:20 (w/v) for 2 h at 65°C with continuous shaking at 200 ×g and centrifuged at 5000 ×g at 4°C for 10 min. The supernatant was collected, concentrated under decreased pressure using a rotary evaporator at 40°C, and mixed with the same amount of 1% (w/v) calcium chloride solution. The combination was incubated overnight at 4°C to precipitate alginate. After centrifugation at 5000 ×g for 10 min, the supernatant was treated with 30% (v/v) ethanol and stored overnight at 4°C. To precipitate fucoidan, the supernatant was further mixed with 70% (v/v) ethanol and incubated overnight at 4°C, then centrifuged for 10 min at 5000 ×g. Sequentially, we used ethanol and acetone to wash the precipitated fucoidan and dried it at room temperature (Govindaswamy *et al*., 2018).

Preparing zein

To extract zein, 50 g of dried corn flour was suspended in 500 mL of 70% (v/v) preheated ethanol solution (60°C) and stirred magnetically at 300 ×g in an Erlenmeyer flask equipped with a cold-water condenser to minimize ethanol loss. The extraction was carried out for 2 h in a water vapor bath. The mixture was centrifuged at 5000 ×g for 10 min and the supernatant was collected. The ethanol was removed from the supernatant using a rotary evaporator at 40°C, and the zein was dried under vacuum and stored at 4°C (Shukla *et al*., 2000).

Biosynthesis of titanium dioxide (TiO_2) nanoparticles from Sargassum tenerrimum extract

Preparation of Algal Extract: Algal cultures were centrifuged for 10 min at 2500 ×g to obtain algal biomass. We washed the biomass twice with distilled water and then dried it for 24 h in a 60°C oven. One gram of dried algal powder was boiled at 100°C in 10 mL of double-distilled water for 15 min in a 100 ml Erlenmeyer flask. The extract was filtered through Whatman No. 1 filter paper and cooled to room temperature. Biosynthesis Reaction: For the biosynthesis of TiO_2 nanoparticles, 10 mL of the algal extract was combined with 90 mL of 1 mM titanium(IV) oxysulfate solution (prepared by dissolving $TiOSO_4$ in distilled water and modifying the pH to 2.0 with 1 M HCl). The combination was stirred magnetically at 300 ×g and maintained at 80°C for 4 h under reflux conditions. We monitored the pH of the reaction mixture and maintained it at 2.0 throughout the synthesis. The color change from pallid yellow to white displayed the formation of TiO_2 nanoparticles. The mixture was then left to cool to room temperature and centrifuged for 15 min at 10,000 ×g to collect the nanoparticle precipitate. We washed the precipitate 3 times with distilled water and 2 times with ethanol to remove unreacted materials and dried it in an oven for 12 h at 80°C. Eventually, we calcined the dried powder in an electric furnace for 2 h at 400 °C to obtain crystalline TiO_2 nanoparticles (Vasanth *et al*., 2022; Alarif *et al*., 2023).

Characterization of TiO_2 nanoparticles

Visible-ultraviolet (UV-Vis) spectroscopy

The optical properties of the synthesized TiO_2 nanoparticles were studied using a Shimadzu UV-2600 spectrophotometer (Japan), which was calibrated using a blank cuvette with distilled water before each measurement. After the reaction mixture color changed to white, the absorption spectrum was recorded in the range of 200–800 nm at room temperature, with a scan speed of 400 nm/min and a spectral bandwidth of 1 nm. Every sample was analyzed in triplicate (n=3), and the mean value was reported (Rathod and Waghuley, 2015).

Zeta potential analysis and dynamic light scattering (DLS)

The hydrodynamic diameter and zeta potential of the colloidal TiO_2 nanoparticles were assessed by applying a Malvern Zetasizer Nano ZS (Malvern Instruments, U K), calibrated with polystyrene latex standards (100 nm, Malvern). We diluted the samples to 0.1 mg/mL with deionized water and sonicated them for 10 min before measurement. Each measurement was carried out 3 times (n=3), and the mean value was noted (Ragheb *et al*., 2017).

Antioxidant activity assessment via DPPH free radical scavenging

The antioxidant activity of biosynthesized TiO_2 nanoparticles was evaluated using the DPPH (2,2-diphenyl-1-picrylhydrazyl) radical scavenging assay. A 0.1 mL sample was mixed with 3.9 mL of DPPH methanolic solution (0.025 g/100 mL) and incubated in the dark at room temperature for 60 min. Absorbance at 515 nm was

measured using a UV-Vis spectrophotometer (UV-1800, Shimadzu, Japan). Quercetin served as the positive control, and methanol was used as the blank. DPPH radical scavenging (%) was calculated using the following formula (Eq. 1):

$$\% \text{ Inhibition} = 100 \times (A_0 - A) / A_0$$

Where, A_0 is the absorbance of the control and A is the absorbance of the sample at 515 nm (Lafka *et al*., 2011).

Preparation of zein/fucoidan nanocomposite containing TiO_2 nanoparticles

Under constant stirring for 15 min at 300 ×g at room temperature (25±2°C), zein (4% w/v) was dissolved in distilled water. Then we added glycerol as a plasticizer at 30% (w/w) of zein and stirred for an additional 10 min. Fucoidan was added at concentrations of 0%, 2.5%, and 5% (w/v) relative to the total solution volume. After that, we homogenized the composite solutions for 30 min, applying a high-speed magnetic stirrer (IKA, Germany) at 500 ×g. TiO_2 nanoparticles were incorporated at an ultimate concentration of 0.5% (w/v) and dispersed by ultrasonication (Sonics Vibra-Cell, USA) at 20 kHz for 10 min. The resulting mixtures (15 mL each) were cast into circular plastic plates (diameter: 9 cm) and dried for 24 h at 25°C. We peeled the films that were dried manually and stored them in a desiccator with 50% relative humidity at 25°C until subsequent analysis. All film formulations were prepared in triplicate (n=3). The treatments studied are summarized in Table 1.

Table 1: The treatments studied in the present study.

Treatment code	Treatment description
Ze	Zein film
Ze/2.5 Fu	Zein/Fucoidan (2.5%) composite
Ze/5 Fu	Zein/Fucoidan (5 %) composite
Ze/2.5 Fu / 2.5TiO_2	Zein/Fucoidan (2.5%) nanocomposite containing 2.5% TiO_2

Characterization of zein/fucoidan/TiO_2 nanocomposite films

Thickness measurement

Applying a digital micrometer (Mitutoyo, Japan) with an accuracy of 0.001 mm, the film thickness was measured. Three measurements were taken at different locations on each film, and the mean value was used for subsequent calculations (Alizadeh-Sani *et al*., 2021).

Solubility

We specified film solubility by placing pre-weighed film samples (2 cm×2 cm, initial dry weight) in a desiccator with calcium chloride (0% relative humidity) for 24 h, followed by immersion in 100 mL deionized water for 24 h at room temperature. Samples were gently agitated for 10 min every 4 h. Next, the undissolved film fragments were filtered, dried at 30°C to a constant weight, and subsequently weighed. The solubility (%) was then calculated using the following formula (Maizura *et al*., 2008):

$$\% \text{ solubility} = (\text{initial film dry weight} - \text{final film dry weight}) / (\text{initial film dry weight}) \times 100$$

Every measurement was done three times (n=3).

Water vapor permeability (WVP)

We measured water vapor permeability according to ASTM E96 and sealed glass vials (diameter: 2 cm) containing 3 g anhydrous calcium chloride with the film samples and put them in a desiccator with 55% relative humidity (magnesium nitrate saturated solution) at 25°C then, we weighed the vials at 2-hour intervals for 24 h using a digital balance (accuracy: 0.0001 g). The gradient of the weight gain is in contrast with the time curve and was used to compute the WVTR, *i.e.,* water vapor transmission rate and WVP was computed as:

$$\text{Water vapor permeability} = \frac{\text{WVTR}\times\text{X}}{\text{P}\times \Delta R}$$

WVTR: Water vapor penetration rate in g/m^2; X: film thickness in meters; P: pure water vapor pressure at ^{o}C 25 in pascals; ΔR: humidity discrepancy between in and out of the vial in percentage. All tests were performed in triplicate (n=3)

Oxygen permeability

Oxygen Permeability was measured based on ASTM D3985-05. Films (area: 5 cm^2) were mounted in diffusion cells at 25°C and 50% relative humidity. Oxygen permeability coefficients were determined using a coulometric sensor (Mocon Ox-Tran 2/21, USA) with 21% oxygen as the test gas and H_2/N_2 as the carrier gas. Steady-state measurements were recorded, and permeability coefficients were calculated considering film thickness. Each sample was tested in triplicate (ASTM, 2002).

Mechanical properties

Mechanical properties were assessed by a texture analyzer (Stable Micro Systems TA.XTplus, UK) equipped with a 1 kN load cell. At a crosshead speed of 50 mm/min, we tested the film strips (150×50 mm). There were five replicates tested for each film type (n=5). Then we computed elongation at break (%) and tensile strength (MPa) based on ASTM D882-08 (ASTM, 2002).

Antibacterial activity of TiO_2 nanoparticle-containing composites

Preparation of bacterial inoculum

Aeromonas hydrophila, Pseudomonas aeruginosa, Yersinia enterocolitica, and Vibrio cholerae strains were obtained from the Iranian Biological Resource Center and cultured on brain heart infusion (BHI) agar at 35±2°C. Bacterial suspensions were prepared by adjusting the optical density at 600 nm to 0.1 (almost 1×10^7 CFU/mL) using a Milton Ray spectrophotometer (USA), which was calibrated with a standard blank before use. The concentration of the cell was confirmed through plate counting on nutrient agar.

Disk diffusion assay

100 µl of bacterial suspension was inoculated onto the Mueller-Hinton agar plates and spread evenly. Composite film disks (diameter: 10 mm, thickness: 0.1 mm) were sterilized by UV irradiation for 30 min and placed at the center of each plate. For 24 h at 37°C, plates were incubated. We measured the diameter of the inhibition zone by applying a digital calliper (accuracy: 0.01 mm) and analysed it with ImageJ software (version 1.46r). A

standard antibiotic disk (gentamicin, 10 µg) was applied as a positive control. Every assay was performed three times (n=3) (Rezaeigolestani *et al*., 2017).

Fourier transform infrared spectroscopy (FTIR)

A Bruker Tensor 27 FTIR spectrometer (Germany) equipped with a ZnSe ATR cell was used to record FTIR spectra. The milled composite samples were placed straight on the ATR crystal, and spectra were obtained within the range of 4000–400 cm^{-1}, utilizing a resolution of 4 cm^{-1}, and averaging 64 scans for each sample. Instrument calibration was performed using a polystyrene film standard (Jiang *et al*., 2020). Every measurement was carried out three times (n=3).

Scanning electron microscopy (SEM)

We analyzed the morphology and elemental composition of the films by applying a Tescan Vega3 SEM (Czech Republic) operated at 15 kV. Samples (2×2 cm) were fixed in 2.5% glutaraldehyde for 2 h, rinsed with acetonitrile, air-dried, and sputter-coated with a 10 nm gold layer (Quorum Q150R ES, UK). Calibration was performed using a copper grid standard (Tongnuanchan *et al*., 2012).

Differential scanning calorimetry (DSC)

We analyzed thermal properties by applying a Mettler Toledo DSC 3+(Switzerland). Almost 4 mg of every sample was sealed in an aluminium pan and heated from 0 to 200°C at a rate of 10°C/min in a nitrogen atmosphere (flow rate: 50 mL/min). We performed instrument calibration using indium and zinc standards. Tg, i.e., the glass transition temperature, was specified from the inflection point of the heat flow curve (Abdollahi *et al*., 2013). Every measurement was done three times (n=3).

Analysis of the statistics

All experimental data are presented as mean ± standard deviation (SD) based on a minimum of 3 independent replicates (n=3), except for mechanical testing, where five replicates (n=5) were used. Statistical analyses were performed utilizing SPSS version 26.0 (IBM, USA). To compare means among various treatments, ANOVA, i.e., one-way analysis of variance, was applied. The assumptions of normality and homogeneity of variances were assessed using the Shapiro-Wilk test and Levene's test, respectively, before performing ANOVA. When significant differences were discovered ($p \leq 0.05$), means were distinguished through Duncan's multiple range test. A considerable level of $p \leq 0.05$ was considered for all statistical tests.

Results

UV–vis spectroscopy analysis of biosynthesized TiO_2 nanoparticles

The UV–Vis absorption spectrum of TiO_2 nanoparticles biosynthesized using *Sargassum tenerrimum* extract (1 mM) showed a distinct SPR, *i.e*., surface plasmon resonance band in the limit of 383±1.5 nm (Fig. 1), which is consistent with the typical absorption range reported for TiO_2 nanoparticles (380–400 nm). This absorption confirms the successful formation of TiO_2 nanoparticles using the algae extract.

Biosynthesized TiO_2 nanoparticles particle size distribution

The dispersion of the biosynthesized TiO_2 nanoparticles, according to the particle size, was determined using DLS, i.e., the dynamic light scattering technique (Table 2; Fig. 2). The results showed a relatively uniform size distribution, indicating the homogeneity of the nanoparticles produced. This uniformity contributes to the stability and potential functionality of the nanoparticles for various applications.

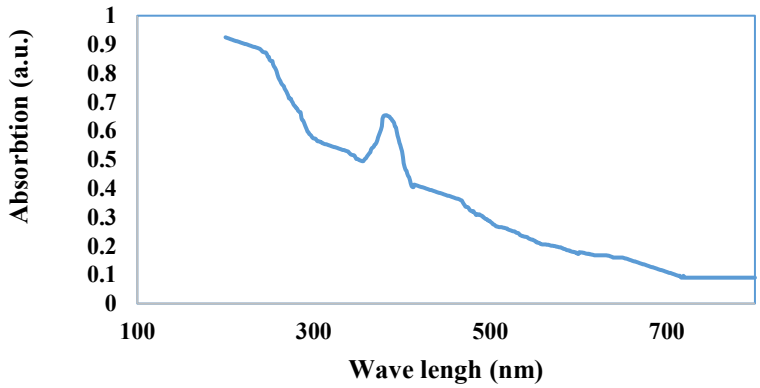

Figure 1: UV-Vis absorption spectrum of TiO_2 nanoparticles biosynthesized using Sargassum tenerrimum extract (1 mM titanium(IV) oxysulfate, pH 2.0, 80°C, 4 h). The surface plasmon resonance (SPR) peak at 383 ± 1.5 nm confirms nanoparticle formation. Measurements were performed in triplicate (n=3) using a Shimadzu UV-2600 spectrophotometer (200–800 nm, scan speed 400 nm/min).

Table 2: Results of particle size distribution by DLS method.

	Particle size (nm)	Amount (%)
Peak (1)	21.06	0.2
Peak (2)	24.36	4.3
Peak (3)	28.21	86.6
Peak (4)	32.67	7.8
Peak (5)	37.84	1.1

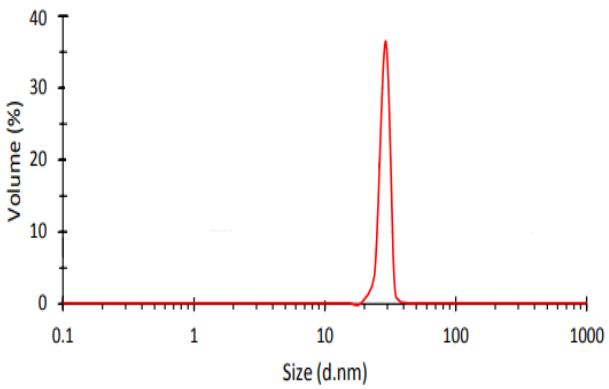

Figure 2: Particle size distribution of biosynthesized TiO_2 nanoparticles determined by dynamic light scattering (DLS) using a Malvern Zetasizer Nano ZS. Samples were diluted to 0.1 mg/mL and sonicated for 10 min before measurement. The narrow distribution indicates high uniformity. Data represent the mean of three replicates (n=3).

Antioxidant activity

The antioxidant potential of green-synthesized TiO_2 nanoparticles using *Sargassum tenerrimum* was assessed via the DPPH radical scavenging assay. The nanoparticles exhibited a moderate antioxidant activity, with an IC_{50} value of 0.347 mg/mL. This suggests that the synthesized nanoparticles possess effective free radical scavenging capability, potentially suitable for active packaging applications.

Physicochemical and mechanical properties of film samples

Thickness

No significant difference was observed in the thickness among the film formulations ($p \geq 0.05$) (Table 3).

Water solubility

The highest water solubility was observed in the Ze sample, while the lowest was recorded in Ze/5Fu/2.5TiO_2 ($p \leq 0.05$) (Table 3).

Water vapor permeability

Ze films showed the highest WVP, whereas Ze/5Fu/2.5TiO_2 exhibited the lowest value ($p \leq 0.05$) (Table 3).

Oxygen permeability

The Oxygen Permeability was significantly higher in Ze films and lowest in Ze/5Fu/2.5TiO_2 ($p \leq 0.05$) (Table 3).

Table 3: The results of thickness, solubility, and permeability to oxygen and water in the film samples.

Sample	Thickness (mm)	Solubility in Water (%)	Permeability to Oxygen (meq/kgO2)	Permeability to Water Vapor ($g \cdot s^{-1} \cdot Pa^{-1} \cdot m^{-1}$)
Ze	0.155 ± 0.01 a	2.05 ± 0.10 a	4.41 ± 0.07 a	0.99 ± 0.01 a
Ze/2.5 Fu	0.155 ± 0.01 a	1.77 ± 0.03 b	4.30 ± 0.10 a	0.94 ± 0.00 b
Ze/5 Fu	0.157 ± 0.01 a	1.65 ± 0.10 b	4.00 ± 0.10 b	0.88 ± 0.02 d
Ze/2.5 Fu/2.5 TiO_2	0.157 ± 0.01 a	1.00 ± 0.08 d	3.93 ± 0.05 b	0.83 ± 0.00 e
Ze/5 Fu/2.5 TiO_2	0.157 ± 0.01 a	1.44 ± 0.03 c	4.00 ± 0.10 b	0.91 ± 0.01 c

Different lowercase letters (a, b, c, d) indicate significant statistical differences ($p<0.05$).
Ze: Zein film, Fu: Fucoidan

Elongation at break (EAB)

Ze and Ze/2.5Fu films demonstrated the lowest EAB, while Ze/2.5Fu/2.5TiO_2 had the greatest flexibility ($p \leq 0.05$) (Table 4).

Tensile strength

TS was lowest in Ze and Ze/2.5Fu films, and highest in Ze/2.5Fu/2.5TiO_2 ($p \leq 0.05$) (Table 4).

Young's modulus

The highest YM was observed in Ze and Ze/2.5Fu films ($p \leq 0.05$) (Table 4).

Antimicrobial activity (inhibition zone diameter)

The nanocomposite films' antimicrobial activity was evaluated based on the diameter of the inhibition zones (mm) formed around the film discs (Table 4). The lowest antimicrobial effect was observed in Ze and Ze/2.5Fu films, while the largest inhibition zones were recorded for Ze/5Fu/2.5TiO_2, followed by Ze/2.5Fu/2.5TiO_2 ($p \leq 0.05$).

Analysis of FTIR, i.e. fourier transform infrared

The FTIR spectra (Fig. 3) confirmed the characteristic functional groups of zein and fucoidan in the respective film formulations. It was evident that the hydrogen bonds were formed and that there were physical interactions between zein and fucoidan, indicating successful incorporation into an organic composite structure. Additionally, the spectra revealed peaks corresponding to TiO_2 nanoparticles, confirming their presence in the nanocomposite films.

Table 4: Inhibition zone diameters (mm) of nanocomposite samples against different bacteria.

Sample	*Vibrio cholerae*	*Yersinia enterocolitica*	*Aeromonas hydrophila*	*Pseudomonas aeruginosa*
Ze	5.00 ± 0.00 d	5.00 ± 0.00 d	5.00 ± 0.00 d	5.00 ± 0.00 d
Ze/2.5 Fu	5.33 ± 0.70 d	5.66 ± 0.70 d	5.33 ± 0.70 d	5.00 ± 0.70 d
Ze/5 Fu	6.66 ± 0.72 c	6.33 ± 0.72 c	6.66 ± 0.72 c	5.66 ± 0.72 c
Ze/2.5 Fu/2.5 TiO_2	9.66 ± 0.72 b	10.33 ± 0.72 b	9.66 ± 0.72 b	7.66 ± 0.72 b
Ze/5 Fu/2.5 TiO_2	13.33 ± 0.72 a	14.33 ± 0.72 a	13.33 ± 0.72 a	11.00 ± 0.72 a

Different lowercase letters (a, b, c, d) indicate significant statistical differences (p<0.05).
Ze: Zein film, Fu: Fucoidan

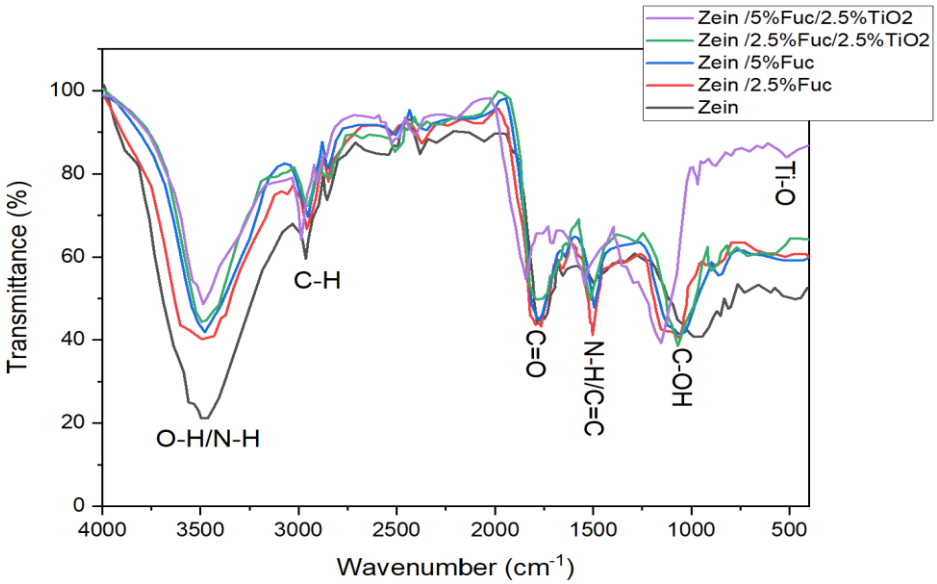

Figure 3: FTIR spectra of zein-based films: (a) pure zein, (b) Ze/2.5Fu, (c) Ze/5Fu, (d) Ze/2.5Fu/2.5TiO_2, and (e) Ze/5Fu/2.5TiO_2. Spectra were recorded using a Bruker Tensor 27 spectrometer (4000–400 cm^{-1}, 4 cm^{-1} resolution, 64 scans). Shifts in peaks (e.g., 1650 cm^{-1} for C=O and below 800 cm^{-1} for Ti–O) indicate hydrogen bonding and TiO_2 incorporation. Measurements were performed in triplicate (n=3).

Differential scanning calorimetry (DSC) analysis

The DSC thermograms of the samples are presented in Figure 4. The pure zein film displayed a glass transition temperature (Tg) at approximately 37.79°C, followed by an endothermic peak in the range of 120–150°C, likely related to the evaporation of residual solvents and water. The incorporation of fucoidan and TiO_2 nanoparticles (except in the Ze/5 Fu/2.5 TiO_2 sample) resulted in a noticeable

growth in both the glass transition temperature and the endothermic peak temperature. These changes indicate improved thermal stability of the nanocomposite films. Among the samples, Ze/2.5 Fu/2.5 TiO_2 exhibited the highest thermal stability, attributed to the synergistic effect of fucoidan at optimal concentration and TiO_2 nanoparticles.

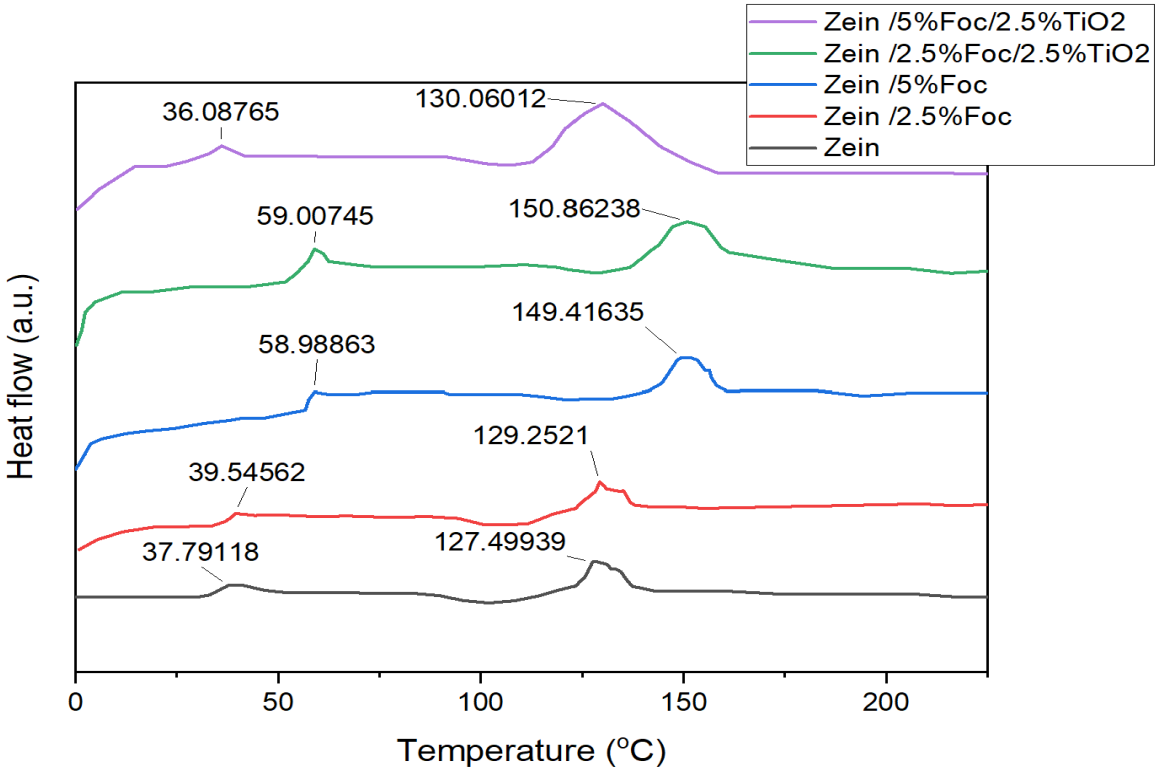

Figure 4: DSC thermograms of zein-based films: (a) pure zein (Tg = 37.79°C), (b) Ze/2.5Fu (Tg = 39.55°C), (c) Ze/5Fu (Tg = 58.99°C), (d) Ze/2.5Fu/2.5TiO_2 (Tg = 59.01°C), and (e) Ze/5Fu/2.5TiO_2 (Tg = 36.09°C). Measurements were conducted using a Mettler Toledo DSC 3+ (0–200°C, 10°C/min, nitrogen atmosphere). The decrease in Tg for Ze/5Fu/2.5TiO_2 suggests phase separation. Data represent the mean of three replicates (n=3).

Scanning electron microscopy (SEM) analysis

The SEM micrographs of the samples are shown in Figure 5. The pure zein film displayed an even surface with no visible secondary phases, indicating the high purity of the film. Upon incorporation of 2.5% (w/w) fucoidan, small particles appeared on the film surface with an average diameter of 0.46±0.23 µm. Increasing the fucoidan concentration to 5% resulted in the formation of slightly larger particles (0.55±0.31 µm), although the difference was not statistically significant due to overlapping standard deviation values. The addition of TiO_2 nanoparticles significantly altered the surface morphology. In the Ze/2.5 Fu/2.5 TiO_2 sample, the average particle size increased to 1.62±0.94 µm, while in the Ze/5 Fu/2.5 TiO_2 sample, it reached 2.03±1.46 µm. These changes confirm the successful incorporation and dispersion of TiO_2 nanoparticles within the film matrix, though with some degree of repletion.

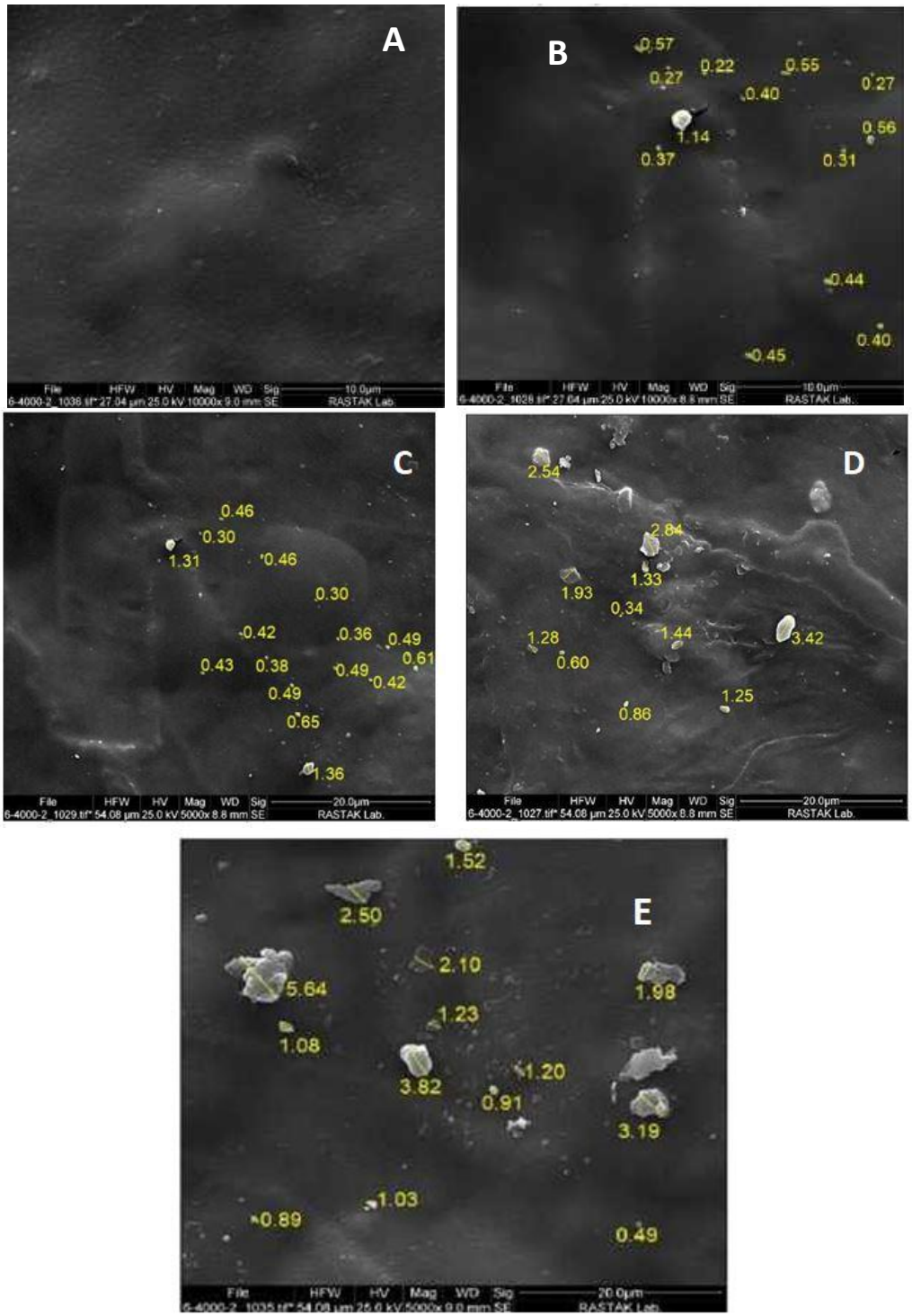

Figure 5: SEM micrographs of zein-based films: (a) pure zein (smooth surface), (b) Ze/2.5Fu (particles: 0.46±0.23 µm), (c) Ze/5Fu (particles: 0.55±0.31 µm), (d) Ze/2.5Fu/2.5TiO₂ (particles: 1.62±0.94 µm), and (e) Ze/5Fu/2.5TiO₂ (particles: 2.03±1.46 µm). Images were obtained using a Tescan Vega3 SEM at 15 kV after gold coating. Particle size increase with TiO₂ indicates organic-inorganic composite formation. Scale bar: 5 µm.

Discussion

In the present study, the surface plasmon resonance (SPR) absorption band of biosynthesized TiO_2 nanoparticles appeared in the span of 383±1.5 nm, confirming their formation. TiO_2 nanoparticles typically exhibit absorption between 380–400 nm, depending on their size, shape, and dispersion in aqueous solution (Santhoshkumar, 2014). The observed SPR band in this study falls within this expected range, supporting the successful green synthesis of TiO_2 using *Sargassum tenerrimum* extract. A spectrophotometer enables the quantitative tracking of nanoparticle formation; an increase in the characteristic absorption peak over time indicates nanoparticle generation during incubation. Similarly, Ahmad *et al*. (2020) reported a peak at 400 nm using mint leaf extract, and Santhoshkumar *et al*. (2020) observed a peak at 380 nm using guava extract. Dahoumane *et al*. (2016) proposed that macromolecules, particularly polysaccharides, may contribute to the stabilization and regeneration of nanoparticles.

Dynamic Light Scattering (DLS) measures the hydrodynamic diameter of particles by analyzing fluctuations in scattered light intensity, which are caused by Brownian motion. This technique accounts for the solvent layer surrounding the particles, resulting in a measured size larger than the core size observed with methods like Transmission Electron Microscopy (TEM). Particle aggregation can further increase the reported size, as DLS may interpret clusters as larger single particles. DLS data are commonly presented in three distributions: intensity, which weights larger particles more heavily; volume, which shows the relative volume of particles; and number, which counts particles across sizes. These distributions are crucial for assessing polydispersity and suspension stability, aiding in the optimisation of synthesis and application processes (Santos *et al*., 2018). In this study, DLS analysis displayed a narrow particle size distribution in the synthesized nanoparticles, indicating high uniformity. This uniformity is particularly important for applications such as food packaging or aquaculture, where size-dependent properties like colloidal stability, permeability, or active agent delivery efficiency are critical. For instance, in food packaging, uniform particle size can enhance barrier properties, while in aquaculture, it can improve nutrient or drug delivery. The precise characterization afforded by DLS confirms the high quality of the nanoparticle preparation and underscores the technique's importance in nanotechnology research, especially when combined with careful sample preparation and consideration of factors like particle shape and concentration (Filippov *et al*., 2023).

The antioxidant activity of green-synthesized TiO_2 nanoparticles using *Sargassum tenerrimum* was evaluated by the DPPH radical scavenging assay, revealing an IC_{50} value of 0.347 mg/mL. This result demonstrates a moderate antioxidant potential when compared to TiO_2 nanoparticles synthesized using other plant extracts. For instance, Rani *et al*. (2022) reported a significantly lower IC_{50} value of 0.0758 mg/mL for TiO_2

nanoparticles synthesized with *Kigelia africana* leaf extract, indicating a stronger radical scavenging ability. Similarly, Blessymol *et al*. (2024) found that TiO_2 nanoparticles derived from *Curcuma longa*, *Myristica fragrans*, and *Kaempferia galanga* exhibited dose-dependent antioxidant activity, with *Curcuma*-based nanoparticles showing the highest efficiency, attributed to the rich phenolic content of the extract. These comparisons suggest that the antioxidant efficiency of TiO_2 nanoparticles largely depends on the phytochemical profile of the plant extract used during synthesis. The TiO_2 nanoparticles obtained from *Sargassum tenerrimum* exhibit a competitive antioxidant capacity, positioning them as promising candidates for application in active food packaging systems aimed at reducing oxidative spoilage.

Our findings indicate that no significant statistical difference was seen in the thickness of the film samples. The thickness of the film is also a factor that determines many mechanical and physical features of the film and affects the mechanical features and also the water vapor permeability of the films (Galdeano *et al*., 2013). The thickness of the films depends on the dry substance of the solution, the primary amount of solution per unit area, the speed of pouring the solution on the surface and the drying conditions. It seems that the differences in those parameters were negligible in film production (da Silva *et al*., 2012; Marismandani and Husni, 2020). Pouralkhas *et al*. (2023), in the preparation of biodegradable films with fucoidan and fish gelatin extracted from *Sargassum tenerrimum,* stated that the average thickness of the layers varied from 0.12 to 0.147 mm.

Results indicate that the highest solubility in water was observed in Ze, and the lowest solubility in water was found for Ze/5 Fu/2.5 TiO_2 ($p \leq 0.05$). Water Solubility is a significant factor in food packaging. Higher solubility indicates greater degradability and less resistance to water. Conversely, solubility affects the release rate of functional compounds (de Souza *et al*., 2024).

The presence of TiO_2 nanoparticles can increase the structural stability of the films due to their crystalline structure and physical properties (Xiao *et al*., 2022). This stability can lead to a decrease in solubility because less material dissolves in the medium, thereby increasing the film's resistance to water. The incorporation of TiO_2 nanoparticles can enhance intermolecular bonds in the film matrix, reducing permeability to water vapor and other liquids (Li *et al*., 2023). The improvement in mechanical strength and barrier properties observed in the zein/fucoidan/TiO_2 nanocomposite films is consistent with previous studies on biopolymer-based packaging films, which report enhanced performance due to the incorporation of functional additives (Nair *et al*., 2023). While the reduction in solubility improves water resistance, it may also affect the release kinetics of active agents, potentially limiting their bioavailability on food surfaces. This dual effect should be further investigated, considering the balance between barrier properties and functionality in active packaging systems. Unexpectedly, some

nanocomposite films may exhibit heterogeneous nanoparticle distribution, which can locally affect solubility and performance; therefore, microstructural characterization is recommended to better understand these effects (Xiao *et al*., 2022). In this study, the highest permeability to water vapor was found for Ze, and the lowest permeability to water vapor was observed in Ze/5 Fu/2.5 TiO. Packaging materials should have the minimum permeability to water vapor as much as possible to curb the exchange of moisture between the environment and food. Transferring water vapor from films is dependent on the permeability and solubility of water molecules in the film matrix (Long *et al*., 2023). The more intermolecular hydrogen bonds between the chains and strong covalent crosslinks in the polymer structure, the greater the cohesion of the polymer matrix. Therefore, the cohesion and integrity of the film increase and its sensitivity to moisture penetration reduces (Li *et al*., 2019; Ponnusamy and Mani, 2022). Titanium oxide nanoparticles can reduce water vapor permeability by creating stronger bonds between polymer chains and increasing the density of the film matrix. By strengthening the structure of the polymer, these nanoparticles prevent moisture from entering the film and, as a result, maintain the quality of packaged food. Also, the presence of TiO_2 nanoparticles can lead to the creation of physical barriers against the movement of water molecules, which also helps to reduce permeability. He *et al*. (2017) stated that the addition of TiO_2 nanoparticles reduced the permeability of the film to water vapor. Meindrawan *et al*. (2020) contended that the addition of zinc oxide nanoparticles at the rate of 3% caused an important reduction in the transfer to water vapor of gelatin bionanocomposite film containing chitin and zinc oxide nanoparticles.

In this paper, the Ze film demonstrated the greatest oxygen permeability, whereas the Ze/5 Fu/2.5 TiO_2 composite exhibited the lowest permeability. Controlling gas permeability is vital for maintaining food quality, as it reduces the loss of volatile compounds and prevents the ingress of environmental gases such as oxygen and carbon dioxide (Ponnusamy and Mani, 2022). Titanium dioxide nanoparticles enhance the polymer network by forming strong crosslinks that increase film density and reduce free volume, thereby limiting oxygen diffusion. This densification also correlates with improved mechanical strength, which supports the barrier function of the films (Ponnusamy and Mani, 2022). Additionally, TiO_2 nanoparticles act as physical obstacles within the matrix, creating tortuous pathways for gas molecules and further decreasing permeability (Li *et al*., 2019). Althogh the effectiveness of this barrier is related to the uniform dispersion of nanoparticles, agglomeration can create defects that increase gas permeability, an aspect requiring careful optimization during film fabrication. Although these results align with prior studies (Ponnusamy and Mani, 2022), discrepancies in oxygen barrier performance may arise from differences in nanoparticle content, crosslinking degree, and processing methods. Thus, optimizing these parameters is essential to maximize the films' protective properties without

adversely affecting flexibility or other functional traits.

The mechanical features of packaging materials are very significant, especially for preserving foods from the environment and knowing little information about the mechanical indicators (tensile strength and percentage of length increase at the moment of rupture) of biodegradable biofilms for designing the packaging process and predicting their ability are very important in maintaining their integrity during their use as packaging material (Ghasemlou *et al*., 2011). For this reason, in the current research, tensile strength (TS: strength), Young's modulus (YM: stiffness), and elongation at break (EAB: flexibility) of the film samples were investigated. Former studies have indicated that the interactions of composite films together with the structural order affect their mechanical properties (Ezati and Rhim, 2020).

In the present study, the lowest elongation at break (EB) was observed for Ze and Ze/2.5 Fu films, while the highest EB value was recorded for the Ze/2.5 Fu/2.5 TiO_2 nanocomposite. Elongation at break, a critical mechanical property for polymeric materials, reflects a film's ability to deform plastically before fracture and is expressed as the percentage increase in length relative to the original dimension. This parameter significantly influences material performance in applications requiring flexibility, such as food packaging (Dey *et al.,* 2021). These findings align with studies on polysaccharide-protein composites. For instance, Pouralkhas *et al*. (2023) reported that incorporating fucoidan into fish gelatin films extracted from *Sargassum tenerrimum* reduced tensile strength from 27.27 to 3.46 MPa, highlighting the trade-off between strength and flexibility in biopolymer composites. Similarly, Kariminejad *et al*. (2018) demonstrated that increasing SiO_2 nanoparticle content (0–1.5%) and polyvinyl alcohol ratio in gelatin-PVA films enhanced elongation at break, emphasizing the role of nanoparticle dispersion and polymer-nanoparticle interactions in improving flexibility. The superior flexibility of the Ze/2.5 Fu/2.5 TiO_2 film suggests that TiO_2 nanoparticles act as plasticizing agents at optimal concentrations, reducing brittleness while maintaining structural integrity. This behavior is consistent with nanocomposite studies showing that well-dispersed nanoparticles can mitigate stress concentration points and improve ductility (Maillard *et al*., 2012' Gupta and Norkey, 2024).

In the present study, Ze and Ze/2.5 Fu films exhibited the lowest tensile strength, while the Ze/2.5 Fu/2.5 TiO_2 nanocomposite demonstrated the greatest tensile strength. Elongation at break (EB) denotes the ability of a material to deform before rupture. Recent studies have shown that excessive nanoparticle loading or agglomeration can deteriorate tensile strength by disturbing the polymer matrix structure (Bhatnagar *et al*., 2024). Overall, these findings confirm that the mechanical properties of nanocomposite films depend strongly on nanoparticle type, concentration, dispersion quality, and interactions with the polymer matrix. Optimizing these factors is essential to maximize tensile strength and film performance for packaging food and other applications.

The Young's modulus, an indicator of film stiffness, was found to be highest for Ze and Ze/2.5 Fu samples. Young's modulus, or the modulus of elasticity, describes the relationship between strain and stress in linear elastic solids below the yield strength, where Hooke's law is applied and the elastic modulus remains constant. It quantifies the force required to deform an elastic material (Kosky *et al*., 2021). These findings align with studies demonstrating that uniform nanoparticle distribution and strong polymer-nanoparticle interactions enhance the mechanical strength of nanocomposites (Hashemi *et al*., 2015). For instance, Rostami Abolwardi *et al*. (2023) investigated polyvinyl alcohol and hydroxypropyl methyl cellulose coating films with varying nano-silver concentrations (1000, 2000, and 4000 ppm). They observed that nano-silver addition up to 2000 ppm did not significantly affect Young's modulus. However, a higher concentration (4000 ppm) resulted in a reduction in Young's modulus, weakening the films, possibly due to nanoparticle aggregation disrupting the polymer matrix. This highlights the significance of optimizing nanoparticle concentration to gain the desired mechanical properties.

Recent improvements in the expansion of zein-based nanocomposites have demonstrated significant improvements in mechanical, barrier, and bioactive features, making them promising candidates for active food packaging usages. The incorporation of natural polysaccharides such as fucoidan into zein matrices enhances film strength and antioxidant capacity through intermolecular hydrogen bonding and synergistic effects (Garavand *et al*., 2024). For instance, Garavand and colleagues (2024) comprehensively reviewed zein nanoparticles and highlighted their potential to improve water vapor barrier and mechanical features, which are critical for preserving food quality. Moreover, titanium dioxide (TiO_2) nanoparticles have been widely discussed for their antimicrobial properties due to their photocatalytic activity that generates reactive oxygen species capable of disrupting bacterial cell walls (Zhang *et al*., 2017; Khan *et al*., 2020). Recent studies have confirmed that TiO_2 nanocomposites incorporated into biopolymer films effectively inhibit common foodborne pathogens like *Escherichia coli* and *Staphylococcus aureus*, while simultaneously enhancing mechanical strength and reducing moisture permeability (He *et al*., 2017; Lin *et al*., 2020). The synergistic integration of zein-fucoidan biopolymers with TiO_2 nanoparticles offers a multifunctional approach to active packaging by combining improved mechanical and barrier features with potent antioxidant and antimicrobial activities. This aligns with the current trend in nanotechnology-enabled packaging of food, aiming to increase shelf life and ensure safety while maintaining environmental sustainability (Li *et al*., 2023). However, despite promising laboratory-scale results, further research is necessary to evaluate the scalability, cost-effectiveness, and long-term stability of these nanocomposites in real-world packaging conditions. Furthermore, it is important to acknowledge the limitations of the current study. The antimicrobial activity

was evaluated in controlled laboratory conditions, which might not fully represent the actual food packaging environment. Future studies should focus on testing the efficiency of these films in actual food systems and under industrial processing conditions. Additionally, economic analyses and life cycle assessments would provide a noteworthy understanding of the feasibility of commercial applications.

Attenuated total reflectance fourier transform ınfrared (ATR-FTIR) spectroscopy was used to investigate the molecular interactions and chemical structures within the zein-based films and their composites. The characteristic absorption peaks observed in the spectra correspond to specific functional groups present in the film components, in line with the former studies (Liu *et al*., 2022). A broad absorption band between 3000 and 3600 cm^{-1} is ascribed to the stretching vibrations of O–H and N–H bonds, which exist in both zein and fucoidan structures (Piai *et al*., 2011; Dai *et al*., 2016). The pure zein film exhibited the most intense peak in this region, primarily due to its abundant amine groups. Upon the incorporation of fucoidan and TiO_2 nanoparticles, a noticeable decrease in peak intensity and narrowing of the band were observed. This change suggests the formation of hydrogen bonds between the amine groups of zein and the hydroxyl groups of fucoidan, which restricts vibrational freedom and indicates strong intermolecular interactions. Similar hydrogen bonding interactions have been reported in zein-polysaccharide composites (Lin *et al*., 2020; Liu *et al*., 2022). The summits observed in the 2750–3000 cm^{-1} range correspond to the asymmetric and symmetric stretching vibrations of C–H bonds in methyl and methylene groups (Nandiyanto *et al*., 2019). These peaks were more pronounced in the pure zein sample compared to the composites, reflecting the higher relative content of C–H bonds in zein (Luo *et al*., 2011; Ali *et al*., 2014). The reduction in intensity in composite films indicates partial replacement or interaction of zein's hydrophobic groups with fucoidan and TiO_2. A distinct peak near 1650 cm^{-1} is associated with the carbonyl (C=O) stretching vibration in zein (Hao *et al*., 2020). This summit remained relatively stable with increasing the concentration of the fucoidan but shifted to higher wavenumbers and decreased in intensity upon TiO_2 nanoparticle addition. This shift indicates the interactions between TiO_2 nanoparticles and carbonyl/carboxyl groups via coordination or hydrogen bonding, which is consistent with the previous reports on TiO_2-biopolymer interactions (Lin *et al*., 2020; Xiao *et al*., 2022). The summit near 1500 cm^{-1} corresponds to the bending vibration of N–H bonds and the stretching vibration of aromatic C=C bonds present in zein and fucoidan (Perumal *et al*., 2018; Sadat and Joye, 2020). This peak shifted to higher wavenumbers with increasing TiO_2 concentration, confirming interactions of TiO_2 nanoparticles not only with carbonyl and carboxyl groups but also with fucoidan's functional groups. The absorption band between 900 and 1150 cm^{-1} corresponds to the stretching vibrations of C–OH and C–N bonds (Perumal *et al*., 2018). The shift of the minimum peak towards higher

wavenumbers in fucoidan-containing films indicates hydrogen bonding between fucoidan's polar groups and zein's amino groups, reinforcing the composite network. A new peak appearing below 800 cm^{-1} in films containing TiO_2 nanoparticles is attributed to the stretching vibration of Ti–O bonds, confirming the presence of TiO_2 within the nanocomposites (Chougala *et al*., 2017). Analogous observations were reported by Lin *et al*. (2020) in gelatin-chitosan-TiO_2-Ag composite films, where TiO_2 enhanced intercomponent interactions. The FTIR results confirm the successful insertion of fucoidan and TiO_2 nanoparticles into the zein matrix. The spectral shifts and intensity changes demonstrate strong physical interactions and hydrogen bonding between zein and fucoidan, and coordination interactions involving TiO_2 nanoparticles. These molecular interactions contribute to the formation of a stable organic-inorganic composite, which underlies the improved physicochemical properties of the films.

The thermal properties of pure zein and its composite films containing fucoidan and TiO_2 nanoparticles were evaluated by differential scanning calorimetry (DSC). The DSC thermogram of pure zein displays a glass transition temperature (Tg) at 37.79°C and an endothermic peak at 127.50°C, corresponding to the evaporation of bound water and residual solvents. These values are lower than those accounted for pure zein in the literature (Wang *et al*., 2014), maybe because of the plasticizers or residual moisture in the film, which reduce intermolecular interactions and thus lower Tg. With the addition of 2.5% fucoidan, Tg increases to 39.55°C and the endothermic peak shifts to 129.25°C. This moderate increase suggests that fucoidan interacts with zein chains, possibly through hydrogen bonding, leading to a more stable and less mobile polymer network (Liu *et al*., 2020). Increasing the fucoidan content to 5% results in a further rise in Tg to 58.99°C and the endothermic peak to 149.42°C. This significant increase indicates enhanced intermolecular interactions and improved thermal stability, as fucoidan acts as a cross-linker, reinforcing the zein matrix. Similar effects have been reported for polysaccharide-protein composites (Periyasamy *et al*., 2025). Adding 2.5% TiO_2 nanoparticles to the Zein/2.5% Fucoidan film leads to a remarkable increase in Tg to 59.01°C and the endothermic peak to 150.86°C. This suggests a synergistic effect between fucoidan and TiO_2, where TiO_2 nanoparticles further limit the mobility of polymer chains and enhance the thermal resistance of the film. The making of hydrogen bonds between zein, fucoidan, and TiO_2, as well as possible physical cross-linking, contribute to this improvement (Xiao *et al*., 2022). Interestingly, in the Zein/5% Fucoidan/2.5% TiO_2 sample, Tg drops to 36.09°C and the endothermic peak to 130.06°C. This decrease may be attributed to the excessive amount of fucoidan, which could lead to phase separation or aggregation, reducing the effective interaction between zein and the additives. The excess fucoidan may not participate in network formation, resulting in a less stable structure (Gelaw and Sarojini, 2020). The Zein/2.5% Fucoidan/2.5% TiO_2 film demonstrates the

highest Tg and endothermic peak, indicating optimal thermal stability due to balanced interactions among all components. Excess fucoidan (5%) in the presence of TiO_2 appears to disrupt the composite network, reducing thermal stability, which is consistent with literature reports that excessive polysaccharides can lead to aggregation and weaker matrices (Liu *et al*., 2020). The overall increase in Tg and endothermic peak with moderate additive levels is attributed to enhanced hydrogen bonding and physical cross-linking, while excessive additive content leads to phase separation and reduced stability (Liu *et al*., 2020). The DSC analysis reveals that the incorporation of fucoidan and TiO_2 nanoparticles can significantly enhance the thermal stability of zein-based films, provided that the additive concentrations are optimized. The best performance was observed for the Zein/2.5% Fucoidan/2.5% TiO_2 sample, while excessive fucoidan in the presence of TiO_2 led to reduced stability due to phase separation or aggregation effects.

Examining SEM, i.e., scanning electron microscopic images, provides a critical understanding the microstructure of zein-based films and their composites, revealing the interactions between components and their effects on film morphology and properties. The pure zein film exhibits a smooth and homogeneous surface with no visible secondary phases, indicating high purity and excellent film-forming ability. This study corresponds with findings by Shankar and Rhim (2018), who accounted for similar surface uniformity in chitosan films, highlighting the importance of a crack-free, compact surface for mechanical integrity.

he addition of fucoidan at 2.5 wt% and 5 wt% resulted in the formation of discrete, light-colored particles on the film surface, with average sizes of 0.46 ± 0.23 μm and 0.55 ± 0.31 μm, respectively. Though there is a little growth in particle size with higher fucoidan content, the increase is statistically insignificant, suggesting stable dispersion within the zein matrix. This is consistent with Liu *et al*. (2020), who demonstrated that fucoidan stabilizes zein nanoparticles through electrostatic and hydrogen-bonding interactions, resulting in uniform globular nanostructures averaging 120–150 nm. The larger particle sizes observed in our SEM images likely reflect aggregation at the microscale during film casting, which is common in composite films. Fucoidan's presence is famous for enhancing antimicrobial and antioxidant activity (Periyasamy *et al*., 2025), and its uniform dispersion without significant aggregation is crucial to maintaining film integrity and functionality. The non-significant size increase indicates effective compatibility and interaction between zein and fucoidan, supporting the formation of a stable composite matrix. The addition of 2.5 wt% TiO_2 nanoparticles markedly alters the film morphology. Particle sizes increase substantially to 1.62±0.94 μm and 2.03±1.46 μm for samples with 2.5% and 5% fucoidan, respectively. This over threefold increase compared to fucoidan-only films suggests the making of an organic-inorganic composite structure on the film surface. Xiao *et al*. (2022) similarly reported that TiO_2 nanoparticles reduce porosity and enhance tensile strength and

barrier properties by forming physical connections within the polymer matrix. The aggregation tendency of TiO_2 nanoparticles, as indicated by the high standard deviations, reflects challenges in achieving homogeneous dispersion, which is a common issue in nanocomposite fabrication. The formation of larger particle clusters may enhance UV-blocking and antimicrobial properties (Gelaw and Sarojini, 2020) but could potentially compromise mechanical flexibility if not well controlled. Therefore, optimizing nanoparticle dispersion methods is essential to balance these effects. Our findings are consistent with the literature demonstrating that fucoidan acts as a stabilizing agent for zein nanoparticles, promoting uniform dispersion and enhancing bioactive properties (Liu *et al*., 2020; Periyasamy *et al*., 2025). The insignificant growth in particle size with fucoidan addition suggests strong molecular interactions that prevent excessive aggregation. Conversely, TiO_2 nanoparticles significantly influence film morphology by forming larger composite structures, corroborating results by Xiao *et al*. (2022) and Gelaw and Sarojini (2020). However, the heterogeneity that was observed indicates that dispersion techniques require refinement to avoid compromising film uniformity. Unexpectedly, while TiO_2 addition improves barrier and mechanical properties (Xiao *et al*., 2022), its effect on particle size heterogeneity highlights a trade-off that must be managed. Future work should focus on advanced dispersion methods, such as ultrasonication or surface modification of nanoparticles, to enhance compatibility and reduce aggregation. The SEM analysis reveals that fucoidan incorporation into zein films results in well-dispersed particles without significant size increase, supporting stable composite formation and enhanced functional properties. Adding TiO_2 nanoparticles leads to larger particle clusters indicative of organic-inorganic composite formation, improving certain film properties but introducing heterogeneity. These findings align well with current literature and emphasize the importance of optimizing nanoparticle dispersion to maximize film performance.

Conclusion

In this study, titanium oxide nanoparticles were successfully biosynthesized using *Sargassum tenerrimum* extract and incorporated into zein/fucoidan nanocomposite films. Characterization techniques including, UV-Vis spectroscopy, FTIR, DSC, and XRD confirmed the formation of nanoparticles and their interactions with the polymer matrix. The nanoparticles exhibited significant antioxidant activity (IC50=0.347 mg/mL), which contributed to enhanced functional properties of the films. Although there were no significant statistical differences in film thickness among samples (p>0.05), the zein-based film demonstrated superior water solubility, water vapor permeability, elongation at break, oxygen permeability, and tensile strength compared to the Ze/5 Fu/2.5 TiO_2 nanocomposite, which demonstrated the lowest values. These findings highlight the complex influence of TiO_2 incorporation on the film properties. However, some limitations should be

acknowledged. The study did not assess the long-term stability or the antimicrobial influence of the nanocomposite films under real food storage conditions, which are vital for practical usage. Furthermore, the potential effects of nanoparticle migration and safety aspects were not evaluated and warrant further investigation. From a practical standpoint, the enhanced UV-blocking, antioxidant, and mechanical properties suggest that these nanocomposite films could serve as promising active packaging materials to extend the shelf life of perishable foods. Their biocompatibility and eco-friendly synthesis further support their industrial relevance. For future research, it is recommended to explore the antimicrobial performance of these films against specific foodborne pathogens, assess their biodegradability and safety in food contact scenarios, and optimize nanoparticle loading to balance functional properties with mechanical integrity. Overall, this study contributes to the field by demonstrating a green synthesis approach to the TiO_2 nanoparticles and their effective incorporation into bioactive nanocomposite films, providing a foundation for developing sustainable and multifunctional food packaging solutions.

Conflicts of interest

The authors declare that they have no conflict of interest.

References

Abdollahi, M., Alboofetileh, M., Rezaei, M. and Behrooz, R., 2013. Comparing physico-mechanical and thermal properties of alginate nanocomposite films reinforced with organic and/or inorganic nanofillers. *Food Hydrocolloids*, 32(**2**), 416–424. DOI:10.1016/j.foodhyd.2013.02.006

Ahmad, N., Sharma, S., Alam, M.K., Singh, V.N., Shamsi, S.F., Mehta, B.R. and Fatma, A., 2020. Green synthesis of titanium dioxide nanoparticles using mint leaf extract and their antimicrobial properties. *Journal of Photochemistry and Photobiology B: Biology,* 205, 111850. DOI:10.1016/j.jphotobiol.2020.111850

Alarif, W.M., Shaban, Y.A., Orif, M.I., Ghandourah, M.A., Turki, A.J., Alorfi, H.S. and Tadros, H.R.Z., 2023. Green synthesis of TiO_2 nanoparticles using natural marine extracts of Bostrychia tenella, Laurencia obtusa, *Halimeda tuna*, and *Sargassum filipendula* for antifouling activity. *Marine Drugs,* 21(**2**), 62. DOI:10.3390/md21020062

Ali, Z., Khatri, K., Oh, I., Kim, S.H. and Kim, Zein, 2014. Zein / Cellulose acetate hybrid nanofibers: Electrospinning and characterization. *Macromolecular Research,* 22(**9**), 971–977. DOI:10.1007/s13233-014-2136-4

Alizadeh-Sani, M., Moghaddas Kia, E., Ghasempour, Z. and Ehsani, A., 2021. Preparation of active nanocomposite film consisting of sodium caseinate, ZnO nanoparticles and rosemary essential oil for food packaging applications. *Journal of Polymers and the Environment*, 29(**2**), 588–598. DOI:10.1007/s10924-020-01902-5

ASTM, 2002. Standard test method for tensile properties of thin plastic sheeting, ASTM D882–02. American

Society for Testing and Materials, *West Conshohocken,*1–10.

Bhatnagar, T., Baxi, P., Sharma, K., Nijhawan, G., Jugran, S., Satyanarayana, K., Sharma, L. and Alhadrawi, M., 2024. Unlocking the strength of nanocomposites: Mitigating the impact of nanoparticle agglomeration on tensile performance. E3S Web of Conferences, 588, 01007. DOI:10.1051/e3sconf/202458801007

Blessymol, B., Yasotha, P., Kalaiselvi, V. and Gopi, S., 2024. An antioxidant study of titanium dioxide (TiO_2) nanoparticles against *Myristica fragrans*, *Curcuma longa* and *Kaempferia galanga* extracts. *Results in Chemistry*, 7, 101291. DOI:10.1016/j.rechem.2023.101291

Chen, Y., Wang, Y., He, L., Wang, L., Zhao, J., Yang, Z., Li, Q. and Shi, R., 2024. Zein/fucoidan-coated phytol nanoliposome: Preparation, characterization, physicochemical stability, in vitro release, and antioxidant activity. *Journal of the Science of Food and Agriculture*, 104, 1234–1245. DOI:10.1002/jsfa.13575

Chougala, L.S., Yatnatti, M.S., Linganagoudar, R.K., Kamble, R.R. and Kadadevarmath, J.S., 2017. A simple approach on synthesis of TiO_2 nanoparticles and its application in dye-sensitized solar cells. *Journal of Nano- and Electronic Physics*, 9(**4**), 04005. DOI:10.21272/jnep.9(4).04005

da Silva, M.E.D., Bierhalz, A.C.K. and Kieckbusch, T.G., 2012. Influence of drying conditions on physical properties of alginate films. *Drying Technology*, 30(**1**), 72–79. DOI:10.1080/07373937.2011.620727

Dahoumane, S.A., Mechouet, M., Wijesekera, K., Filipe, C.D.M. and Sicard, C., 2016. Biosynthesis of nanoparticles: A review. *Environmental Chemistry Letters*, 14(**4**), 399–414. DOI:10.1007/s10311-016-0570-4

Dai, C., Sun, D., Wang, Y. and Gao, Y., 2016. The interaction between zein and lecithin in ethanol-water solution and characterization of zein–lecithin composite colloidal nanoparticles. *PLoS One*, 11, e0167172. DOI:10.1371/journal.pone.0167172

de Souza, A.M.N., Avila, L.B., Contessa, C.R., Valério Filho, A., de Rosa, G.S. and Moraes, C.C., 2024. Biodegradation study of food packaging materials: Assessment of the impact of the use of different biopolymers and soil characteristics. *Polymers,* 16(**20**), 2940. DOI:10.3390/polym16202940

Dey, A., Roan Eagle, I.N. and Yodo, N., 2021. A review on filament materials for fused filament fabrication. *Journal of Manufacturing and Materials Processing*, 5(**3**), 69. DOI:10.3390/JMMP5030069

Dukuzeyesu, G., Xu, C. and Yue, Z., 2020. Edible films made of Corn Zein protein and cellulose derivatives. Poster presented at the UCARE Research Fair, University of Nebraska-Lincoln.

Ezati, P. and Rhim, J.W., 2020. pH-responsive chitosan-based film incorporated with alizarin for intelligent packaging applications. *Food Hydrocolloids*, 102, 105629. DOI:10.1016/j.foodhyd.2020.105629

Filippov, S.K., Khusnutdinov, R., Murmiliuk, A., Inam, W., Zakharova, L.Y., Zhang, H. and Khutoryanskiy, V.V., 2023. Dynamic light scattering and transmission electron microscopy in drug delivery: A roadmap for correct characterization of nanoparticles and interpretation of results. *Materials Horizons,* 10(**12**), 5354–5370.

Galdeano, M.C., Wilhelm, A.E., Mali, S. and Grossmann, M.V.E., 2013. Influence of thickness on properties of plasticized oat starch films. *Brazilian Archives of Biology and Technology,* 56(4), 637–644. DOI:10.1590/S1516-89132013000400014

Gelaw, T. B. and Sarojini, B. K., 2020. Improving photocatalytic and antibacterial properties of zein/polyvinyl alcohol polymer composite film by dispersing TiO_2 nano particles. Journal of Organic Polymers and Composites, 8(2), Article 4258. DOI:10.37591/jopc.v8i2.4258

Garavand, F., Khodaei, D., Mahmud, N., Islam, J., Khan, I., Jafarzadeh, S. and Cacciotti, I., 2024. Recent progress in using zein nanoparticles-loaded nanocomposites for food packaging applications. *Critical Reviews in Food Science and Nutrition*, 64(**12**), 3639–3659.

Ghasemlou, M., Aliheidari, N., Fahmi, R., Shojaee-Aliabadi, S., Keshavarz, B., Cran, M. J. and Khaksar, R., 2011. Physical, mechanical and barrier properties of corn starch films incorporated with plant essential oils. *Carbohydrate Polymers***,** 86**(1)**, 459–466**.** DOI:10.1016/j.carbpol.2011.05.010

Govindaswamy, R., Robinson, J. S., Geevaretnam, J., et al., 2018. Physico - functional and anti-oxidative properties of carp swim bladder gelatin and brown seaweed fucoidan based edible films.*Journal of Packaging Technology and Research*, 2, 77–89. DOI:10.1007/s41783-017-0024-z

Gupta, R. and Norkey, G., 2024. Effects of nanoparticle on mechanical properties of epoxy nanocomposites. *International Journal for Research in Applied Science and Engineering Technology,* 12(**9**), 477–483. DOI:10.22214/ijraset.2024.64165

Hao, L., Lin, G., Wang, H., Wei, C., Chen, L., Zhou, H., Chen, H., Xu, H. and Zhou, X., 2020. Preparation and characterization of zein-based nanoparticles via ring-opening reaction and self-assembly as aqueous nanocarriers for pesticides. *Journal of Agricultural and Food Chemistry,* 68(**36**), 9624–9635. DOI:10.1021/acs.jafc.9b06494

Hashemi, A., Jouault, N., Williams, G.A., Zhao, D., Cheng, K.J., Kysar, J., Guan, Z. and Kumar, S.K., 2015. Enhanced glassy state mechanical properties of polymer nanocomposites via supramolecular interactions. *Nano Letters*, 15(**9**), 6179–6184. DOI:10.1021/acs.nanolett.5b02016

He, Q., Liu, Y. and Zhang, Y., 2017. A nanocomposite film fabricated with simultaneously extracted protein-polysaccharide from a marine alga and TiO_2 nanoparticles. *Journal of Applied Phycology,* 29(**5**), 1541–1552. DOI:10.1007/s10811-017-1103-9

Jiang, Y., Zhang, X. and Wang, L., 2020. Qualitative analysis of functional groups of biopolymer composites by Fourier Transform Infrared (FTIR) spectroscopy. *Journal of Materials Science and Ch*emical Engineering, 8(6), 14–22. DOI:10.4236/msce.2020.86002

Kariminejad , M., Nouri, L. and Rouhi, M., 2018. Effect of silica nanoparticles and polyvinyl alcohol content on mechanical and physical properties of gelatin–PVA composite films. ***Journal of Food Processing and Preservation*****,** 42**(6), e13644.** DOI:10.1111/jfpp.13644

Khan, M.A., Raza, M.A. and Khan, S., 2020. Photocatalytic antimicrobial activity of TiO_2 nanoparticles: Mechanism and applications. *Journal of Photochemistry and Photobiology B: Biology,* 204, 111789. DOI:10.1016/j.jphotobiol.2020.111789

Kosky, P.G., Balmer, R.T., Keat, W.D. and Wise, G., 2021. Exploring engineering: An introduction to engineering and design. Academic Press. pp 527-552.

Lafka , T. I., Sinanoglou, V. J. and Lazos, E. S., 2011. On the extraction and antioxidant activity of phenolic compounds from winery wastes .*Food Chemistry,* 124(3), 1208–1211. DOI:10.1016/j.foodchem.2010.07.080

Li, J., Zhang, D. and Hou, C., 2025. Application of nano-titanium dioxide in food Antibacterial packaging materials. Bioengineering, 12(1), 19. DOI:10.3390/bioengineering12010019

Li, X., Liu, Y., Chen, Y., Wang, Q. and Zhang, L., 2019. Effect of TiO_2 nanoparticles on the structure, mechanical and barrier properties of protein-based composite films.Food Hydrocolloids, 95, 477–485. DOI:10.1016/j.foodhyd.2019.04.045

Li, Y., Zhang, M., Liu, X., Chen, H. and Wang, J., 2023. Synergistic effects of TiO_2 nanoparticles on the mechanical, barrier, antioxidant and antimicrobial properties of biopolymer-based nanocomposite films for active food packaging.International Journal of Biological Macromolecules, 241, 124567. DOI:10.1016/j.ijbiomac.2023.124567

Lin, J., Liu, Y. and Chen, X., 2020. Preparation and properties of TiO_2-Ag fish gelatin-chitosan antibacterial composite film. *Food Hydrocolloids,* 108, 106011. DOI:10.1016/j.foodhyd.2020.106011

Liu, Q., Chen, J., Qin, Y., Jiang, B. and Zhang, T., 2020. Zein/fucoidan-based composite nanoparticles for the encapsulation of pterostilbene: Preparation, characterization, physicochemical stability, and formation mechanism. *International Journal of Biological Macromolecules,* 158, 461–470. DOI:10.1016/j.ijbiomac.2020.04.128

Liu, Y., Zhang, Y., Li, X., Wang, L. and Li, J., 2022. Preparation and characterization of zein-based nanocomposite films incorporated with TiO_2 nanoparticles. *Food Hydrocolloids*, *125*, 107389. DOI:10.1016/j.foodhyd.2022.107389

Long, J., Zhang, W., Zhao, M. and Ruan, C.Q., 2023. The reduce of water vapor permeability of polysaccharide-based

films in food packaging: A comprehensive review. *Carbohydrate Polymers,* 321, 121267. DOI:10.1016/j.carbpol.2023.121267

Luo, X.L., Zhu, J.Y., Gleisner, R. and Zhan, H.Y., 2011. Effects of wet-pressing-induced fiber hornification on enzymatic saccharification of lignocelluloses. *Cellulose,* 18(**4**), 1055–1062. DOI:10.1007/s10570-011-9561-2

Maillard, D., Kumar, S.K., Fragneaud, B., Kysar, J.W., Rungta, A., Benicewicz, B.C., Deng, H., Brinson, L.C. and Douglas, J.F., 2012. Mechanical properties of thin glassy polymer films filled with spherical polymer grafted nanoparticles. *Nano Letters,* 12(**8**), 3909–3914. DOI:10.1021/nl301792g

Marismandani, A.D.P. and Husni, A., 2020. Development and characterization of biobased alginate/glycerol/virgin coconut oil as biodegradable packaging. In E3S Web of Conferences, 147, 03016. DOI:10.1051/e3sconf/202014703016

Maizura, M., Fazilah, A., Norziah, M. H. and Karim, A. A., 2008.Antibacterial activity and mechanical properties of partially hydrolyzed sago starch–alginate edible film containing lemongrass oil.*Food Hydrocolloids, 22*(**6**), 1084–1093. DOI:10.1016/j.foodhyd.2007.05.004

Meindrawan, B., Putri, S., Susanto, C.S., Ofe, O., Mangindaan, D., Ayman, A. and Kasih, T.P., 2020. Bionanocomposite of gelatin–ZnO nanoparticles as potential edible coating for broiler chicken fillet. *Macromolecular Symposia,* 391, 1900165. DOI:10.1002/masy.201900165

Nair, M. S., Zhang, J. and Chen, H., 2023. Biopolymer-based edible films and coatings: Toward eco-friendly food packaging. *International Journal of Food Science & Technology*, 58, 4512–4526. DOI:10.1111/ijfs.16034

Nandiyanto, A.B.D., Oktiani, R. and Ragadhita, R., 2019. How to read and interpret FTIR spectroscope of organic material. *Indonesian Journal of Science and Technology*, 4(**1**), 97–118. DOI:10.17509/ijost.v4i1.15806

Nguyen, S.V. and Lee, B.K., 2022. PVA/CNC/TiO_2 nanocomposite for food-packaging: Improved mechanical, UV/water vapor barrier, and antimicrobial properties. *Carbohydrate Polymers*, 295, 120064. DOI:10.1016/j.carbpol.2022.120064

Periasamy, D., Manoharan, B., Arockiasamy, F.S., Karuppiah, P., Periyasamy, B.K., Ranganathan, N. and Dhandapani, A., 2025. Exploring the mechanical and thermal characteristics of polypropylene composites with recycled polyester waste as sustainable reinforcement for enhanced protection in safety helmets ' band. Progress in Rubber, *Plastics and Recycling Technology,* DOI:10.1177/14777606241313076

Perumal, R.K., Perumal, S., Thangam, R., Gopinath, A., Ramadass, S.K., Madhan, B. and Sivasubramanian, S., 2018. Collagen-fucoidan blend film with the potential to induce fibroblast proliferation for regenerative applications. *International Journal of Biological Macromolecules,* 106, 1032–

1040. DOI:10.1016/j.ijbiomac.2017.08.089

Piai, J. F., Farias, N. C., Costa, T. M. H., Guterres, S. S. and Beck, R. C. R., 2011. Zein nanoparticles produced by antisolvent precipitation: A study of particle formation and stability**.** *Journal of Agricultural and Food Chemistry*, **59**, 10035–10041. DOI:10.1021/jf202537n

Ponnusamy, P.G. and Mani, S., 2022. Material and environmental properties of natural polymers and their composites for packaging applications—A review. *Polymers,* 14(**19**), 4033. DOI:10.3390/polym14194033

Pouralkhas, M., Kordjazi, M., Ojagh, S.M. and Farsani, O.A., 2023. Physicochemical and functional characterization of gelatin edible film incorporated with fucoidan isolated from *Sargassum tenerrimum*. *Food Science and Nutrition,* 11(**7**), 4124–4135. DOI:10.1002/fsn3.3402

Qu, L., Chen, G., Dong, S., Huo, Y., Yin, Z., Li, S. and Chen, Y., 2019. Improved mechanical and antimicrobial properties of zein/chitosan films by adding highly dispersed nano-TiO_2. *Industrial Crops and Products,* 134, 289–297. DOI:10.1016/j.indcrop.2018.12.093

Ragheb, A. A., Hameed, M. R., El-Sherbiny, I. M. and El-Morsi, E. A., 2017. Synthesis and characterization of TiO_2 nanoparticles for photocatalytic degradation of organic dyes under UV irradiation. *Journal of Nanomaterials*, 5679817. DOI:10.1155/2017/5679817

Rani, N.U., Pavani, P. and Prasad Rao, P.T.S.R.K., 2022. Facile green synthesis and characterization of titanium dioxide nanoparticles using Kigelia africana (Lam) Benth., aqueous leaf extract and its antioxidant and antibacterial activity. *Asian Journal of Chemistry*, 34(**2**), 409–414. DOI:10.14233/ajchem.2022.23563

Rathod, P. and Waghuley, S.A., 2015. Synthesis and UV-Vis spectroscopic study of TiO_2 nanoparticles**.** *International Journal of Nanomanufacturing*, 11(**3/4**). DOI:10.1504/ijnm.2015.071925

Rezaeigolestani, M., Misaghi, A., Khanjari, A., Akhondzadeh Basti, A., Abdulkhani, A. and Fayazfar, S., 2017. Antimicrobial evaluation of novel poly-lactic acid based nanocomposites incorporated with bioactive compounds in-vitro and in refrigerated vacuum-packed cooked sausages. *International Journal of Food Microbiology*, 260, 1–10. DOI:10.1016/j.ijfoodmicro.2017.08.015

Rostami Abolvardi, F., Nia Kothari, M. and Dadfar, S.M., 2023. Synthesis of hydroxypropyl methylcellulose/polyvinyl alcohol nanocomposite containing silver nanoparticles and investigation of its physicochemical and antimicrobial properties. MSc thesis. Bushehr: Khorram University. (In Persian)

Sadat, A. and Joye, I.J., 2020. Peak fitting applied to Fourier transform infrared and Raman spectroscopic analysis of proteins. *Applied Sciences,* 10(**17**), 5918. DOI:10.3390/app10175918

Santhoshkumar, P., Rajeshkumar, S. and Venkat Kumar, S., 2014. Green synthesis of titanium dioxide nanoparticles using plant extracts and

their photocatalytic activity. *Materials Letters*, 130, 16–19. DOI:10.1016/j.matlet.2014.05.003

Santhoshkumar, P., Venkat Kumar, S. and Rajeshkumar, S., 2020. Biosynthesis of TiO_2 nanoparticles using guava leaf extract and their photocatalytic and antimicrobial activities. *Journal of Environmental Chemical Engineering*, 8(**5**), 104125. DOI:10.1016/j.jece.2020.104125

Santos, M.A., Lima, R.M. and Ferreira, J.F., 2018. Dynamic light scattering: Principles and applications. *Journal of Nanotechnology*, 2018, 1234567. DOI:10.1155/2018/1234567

Shankar, S. and Rhim, J.W., 2018. Bionanocomposite films for food packaging applications. *Reference Module in Food Science*, 1, 1–10.

Shukla, R., Cheryan, M. , 2000. Zein: The industrial protein from corn**.** *Industrial Crops and Products, 13***(3)**, 171–192. DOI:10.1016/S0926-6690(00)00064-9

Tongnuanchan, P., Benjakul, S. and Prodpran, T., 2012. Physical and antimicrobial properties of fish skin gelatin film incorporated with essential oils. *Food Hydrocolloids,* 27(2), 371–379. DOI:10.1016/j.foodhyd.2011.09.011

Vasanth, V.V., Murugesh, K.A. and Susikaran, S., 2022. Synthesis of titanium dioxide nanoparticles using Spirulina platensis algae extract. *The Pharma Innovation Journal*, 11(**7S**), 266–269. DOI:10.17605/OSF.IO/9Z2P6

Wang, T., Lin, J., Chen, Z., Megharaj, M. and Naidu, R., 2014. Green synthesized iron nanoparticles by green tea and eucalyptus leaves extracts used for removal of nitrate in aqueous solution. *Journal of Cleaner Production*, 83, 413–419. DOI:10.1016/j.jclepro.2014.07.015

Xiao, Y., Liu, Y., Wang, Q., Pan, Y. and Lin, C., 2022. Preparation and characterization of zein-based nanocomposite films incorporated with TiO_2 nanoparticles. *Food Hydrocolloids*, 125, 107398. DOI:10.1016/j.foodhyd.2021.107398

Zhang, Y., Liu, Y. and He, J., 2017. Antimicrobial activity of titanium dioxide nanoparticles: A review. *Journal of Nanomaterials*, 1234567. DOI:10.1155/2017/1234567